

## COMPUTER SIMULATION OF LARGE-SCALE WAVE MOTIONS ASSOCIATED WITH THE GENESIS FLOOD†

M. E. CLARK\* AND H. D. VOSS\*

*The theory and numerical methodology is developed whereby the dynamic processes associated with large-scale wave motions in the context of a global flood can be delineated. After a brief review of wave mechanics,‡ the available analytical results are given in synopsis. The basic computer algorithm, SOLA-SURF, is then described and utilized to produce solutions to a series of problems considered to be germane to Genesis Flood explanations. The results of these simulations are presented in terms of the velocity fields and the temporal sequencing of the free-surface configurations. Interpretations of the results leads to inferences as to the development of sedimentary strata left by the passing of the wave motions.*

### 1. Introduction and General Problem Description

A quantitative flood model is crucial to understanding the earth's geologic features from a nonuniformitarian point of view. Such a model should feature dynamic global flow processes and be capable of incorporating the sedimentary processes of erosion, transport and deposition. In the past, bold assertions that large-scale fluid motions were capable of producing large-scale geologic features might have been the only available response to the uniformitarian's equally bold assertions. Now, however, tools have become available by which the complex dynamic processes and mechanisms that were involved during the Genesis Flood can be simulated. It is, therefore, incumbent upon flood catastrophists to attempt to couple flood hydraulics and flood geology and to put them on a quantitative base. If a global flood capable of producing the majority of the earth's sedimentary rocks is fact, then rigorous investigations using the disciplines of hydrodynamics and sedimentology should lead to accurate predictions of extant geological structures and terrain.

In order to pursue these ends, a global flood model of the significant and fundamental processes must be made.<sup>1</sup> Certainly, large global mechanisms are required if one is to suggest that nearly all of the  $4 \times 10^8$  km<sup>3</sup> of sedimentary rock could have been laid down in the incredibly short span of one year. Such a strict catastrophic view is consistent with a literal interpretation of Scripture and is capable of explaining many of the apparent inconsistencies associated with uniformitarianism. Local lithologies could also be better interpreted in terms of such a model by incorporating not only the particularities of the local depositional environment but also the generalities of global occurrences.

Considerable success has been achieved during the past decade in solving practical free-surface transient-flow problems using computer codes based on finite difference (primitive variable) methods.<sup>2</sup> This paper reports on the first use of this type of code for global flood model calculations. The preliminary results of this paper are most important in establishing proce-

dures for depicting likely flow patterns encountered during the motion of large fluid masses. These numerical procedures are not limited to simple bottom boundaries as are the analytical methods. They allow considerable freedom in the choice of sloping and curved bottom boundaries. Changes in bottom surface configuration as a function of time, equivalent to tectonic activity, as well as injection of fluid from such sites of change, equivalent to the opening of the fountains of the deep, can be handled by modification of the boundary conditions. Future modifications to this basic program will allow detailed calculations to be made of erosion, transport, and deposition of a multiconstituent sediment as a function of time over a simulated continent.

It is the main purpose of this paper, then, quantitatively to examine the theory, procedure, and computer code necessary to describe the complex hydrodynamic processes of a global flood. A general background on wave mechanics is followed by a short discussion of the significant but limited analytical solutions for wave propagation characteristics that are available. This work naturally leads into the major portion of the paper which develops the more intricate theory and numerical methodology of flood actions. The basic computer algorithm is first tested by showing that it reproduces problem solutions already in the literature. The algorithm is then modified to simulate some practical flood problems in preliminary fashion. A single wave propagating up a continental incline is first simulated; the case where the same wave propagates over the sequence of a submerged continental incline, mountain region, and mid-continent basin is then analyzed. The final simulations involve two subaqueous activities: the first depicts the flow patterns developed by the rapid injection of water into an ocean basin from an opening in the bottom boundary; the second shows the patterns resulting from a sudden uplift of a portion of an ocean basin. Discussion of these results and relevant conclusions are made in the final selection.

### 2. Background and Basic Wave Mechanic Relations

Many conditions associated with a global flood can be simulated if certain rational assumptions are made about its nature (e.g., the amount of water present, the bottom surface relief, wave mechanisms generating

\*Mr. Clark and Mr. Voss are with The Genesis Research Laboratory, 505 East Green Street, Urbana, Illinois 61801. The Genesis Research Laboratory is concerned with experimental and theoretical investigations of questions which are important to Creationism.

†This report was submitted to the Creation Research Society on work done at The Genesis Research Laboratory, partly supported by a grant from the Society.

‡The term "wave mechanics" is used in this Report to mean the mechanics of waves on water. It has nothing to do with Schrodinger, or with quantum theory.

dynamic motion of the water) and if a method is employed which insures the proper application of the governing laws in the processes that take place in every element of the model. Since analytical solutions for such complex flow fields cannot be generated, the analyst must develop solutions using numerical methods in conjunction with large digital computers. Only recently have computers become large and fast enough to produce realistic results. These computer solutions could, for example, predict the details of the fluid motion in every region of a simulated ocean basin by producing the velocity vector fields, the pressure and shear fields, as well as the history of the changes in the free-surface configuration. This information could then be coupled with the known laws of sedimentology to postulate information regarding the make-up of sedimentary rock in a given region and the manner in which it was laid down to form the earth's crust. The general features of large inland basins (like cyclothems, other layered sequences, or persistent facies) could thus be explained on the basis of the cyclic action associated with global waves.

In this paper, wave motions on both large (global) and small (local) scales are deemed to be the significant mechanisms responsible for the development of the sedimentary geologic column. Although wave motions are omnipresent in the natural world, their basic features are enigmatic to the casual observer. They are, in essence, disturbances which move through a given medium, but do not move it at anywhere near the same rate as they move. A cork, for example, bobbing on the surface as waves pass by, is seen to remain in essentially the same horizontal position.

All the different kinds of waves (water waves, stress waves, radio waves, light waves) obey the same fundamental laws and have similar characteristics. The most significant of these for a water wave are: amplitude  $A$  (height of rise of the wave above the undisturbed free surface), wave length  $L$  (distance between successive

wave crests in a wave train), frequency of occurrence  $f$  or period  $T$ , and the speed of travel  $c$ . The wave speed is related as follows to the wave length, frequency, and/or period:

$$c = L/T \text{ or } c = Lf \tag{1}$$

Waves are greatly affected by changes in the characteristics of the medium. As long as a channel maintains constant cross-section and depth, a given surface wave will travel with constant speed. Should the depth or cross-section change, the wave characteristics change accordingly. Changes in channel cross-section or the interaction of waves with boundaries result in the generation of reflections. The incident and reflected waves interfere to form a resultant wave with modified characteristics.

Oscillatory and translatory waves are the main two types of water waves. In the former, the net mass transport is nil; in the latter, there is a definite amount of fluid advancement in the wave direction. Water waves are also categorized by the relative values of wave length  $L$  and depth  $d$ . In Fig. 1 three ranges of the  $d/L$  ratio for oscillatory waves define as many different situations regarding the manner in which the water reacts to the passing of the disturbance. When the depth of the water is greater than half the wave length, the deep-water condition is present and surface motion (in the form of circular particle orbits) decays exponentially with depth resulting in little or no bottom motion or influence. When the depth is small compared to wave length ( $d/L$  less than 0.05), shallow water waves disturb all of the fluid (orbits are horizontal back-and-forth displacements of particles). At intermediate  $d/L$  ratios, surface effects are again felt throughout the flow depth (ellipses degenerating to a straight line at the bottom). In Fig. 1, the length is scaled with respect to depth for the assumed  $d/L$  values. The particle orbits are also scaled with respect to the wave amplitude; however, since the relations used to calculate the proper propor-

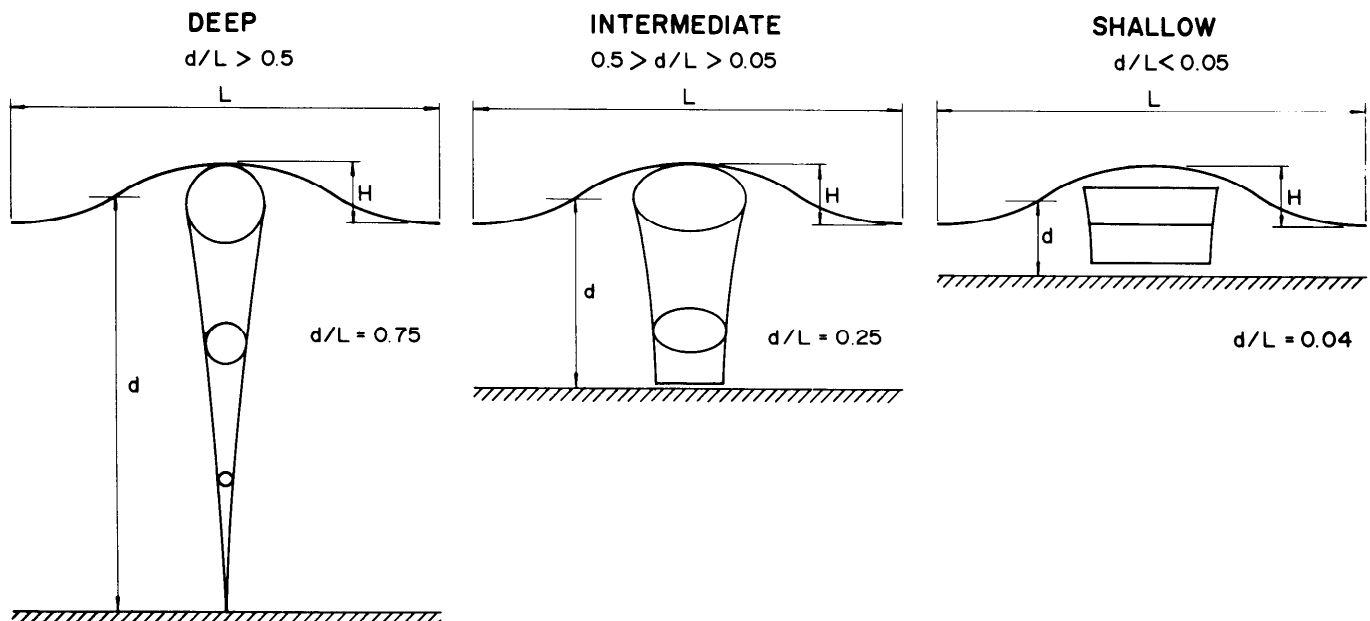


Figure 1. The three categories of water wave characteristics.

tions are based on small-amplitude theory, it is necessary for clarity to exaggerate the amplitude.

Translatory waves are usually characterized by a solitary wave of long length and finite amplitude, and are treated as shallow-water waves. As such, they would manifest the same type of fluid motion beneath the surface as periodic waves. Translatory waves can be generated by subaquatic tectonic activity or by true tidal forces.

### 3. Analytical Solutions for Wave Propagation Characteristics

Before describing the numerical studies based on the general Navier-Stokes governing equations, consideration is here given to some of the results of analytical solutions based on the simpler inviscid Bernoulli governing equations. For horizontal and ramp bottom boundaries, these descriptions of flow can be associated with large global motions and lead to valuable insights into flood dynamics which, in turn, aid in understanding geomorphology. In particular, the description of the velocity field in the vicinity of the bottom boundary is most useful when trying to understand the flow environment associated with the production of sedimentary formations. The analytical methods break down, however, for more complex geometrical boundary configurations and for large-amplitude waves—areas where the numerical methods can still be used.

Stokes, in 1880, developed the theory for progressive periodic waves of small but finite amplitude in a medium of constant depth using expressions for the velocity potential up to the third order (the first order being so-called linear theory). For the first or second order, the speed of wave propagation  $c$  is given by

$$c = \left[ \frac{gL}{2\pi} \tanh \frac{2\pi d}{L} \right]^{0.5} \quad (2)$$

where  $g$  is the gravitational constant,  $L$  the wave length, and  $d$  the depth of the water. For deep water waves ( $d/L > 0.5$ ),  $\tanh (2\pi d/L) \rightarrow 1$  and  $c = [gL/2\pi]^{0.5}$ . For shallow water waves ( $d/L < 0.05$ ),  $\tanh (2\pi d/L) \rightarrow 2\pi d/L$  and  $c = [gd]^{0.5}$ . Using these relations and adopting some reasonable lengths for a global ocean wave, corresponding wave speeds can be calculated. A wave 100 km long would move at a rate of 915 km/hr in an ocean 7 km deep ( $d/L = 0.07$ ) but only 178 km/hr where the depth was 0.25 km ( $d/L = 0.0025$ ). Neither rate is small; but an observer on a ship (or ark) would not be aware of these large speeds since he would merely bob vertically according to the wave amplitude.

The wave amplitude given by Stokes is

$$A = \frac{a}{c} \sinh \left( \frac{2\pi d}{L} \right) = \frac{a \sinh (2\pi d/L)}{[(gd/2\pi) \tanh (2\pi d/L)]^{0.5}} \quad (3)$$

where  $a$  is the generator strength. The variation in wave amplitude with depth is difficult to assess using Eq. 3. In 1911, Rayleigh developed a method for use on uniform periodic waves as they entered shoaling waters. Constancy of wave energy assumed, the ratio of the wave amplitude  $H$  at any depth to the wave amplitude  $H'$  in deep water (i.e., water in which increases in depth no longer affect the wave characteristics) is

$$\frac{H}{H'} = \left[ \frac{1}{2n} \frac{c_0}{c} \right]^{1/2} \quad (4)$$

where

$$n = \frac{1}{2} \left[ 1 + \frac{4\pi d/L}{\sinh 4\pi d/L} \right] \quad (5)$$

The wave speed in water of any depth  $c$  in ratio to that in deep water  $c_0$  is

$$\frac{c}{c_0} = \frac{L}{L_0} = \tanh \frac{2\pi d}{L} \quad (6)$$

Tabulation of these quantities in terms of the  $d/L$  ratio are found in Wiegel.<sup>3</sup> Continuing the foregoing example and using Rayleigh's method, the 100 km wave moving at 915 km/hr with amplitude  $H$  in 7 km of water would have a height of  $0.88H$  in deep water. Its wave length and speed in deep water would be 241 km and 2211 km/hr, respectively. According to the Rayleigh method, when this wave shoaled to a water depth of 0.25 km, the wave would increase its amplitude to  $2.2H$  while decreasing its length to 19.5 km and its speed to 278 km/hr. These results are shown in Fig. 2.

The velocity field associated with first order (linear) theory is given by the horizontal ( $u$ ) and vertical ( $v$ ) component velocities as follows:

$$u = \frac{H}{2} k \frac{\cosh m(d+z)}{\sinh md} \sin(kt - mx) \quad (7)$$

$$v = \frac{H}{2} k \frac{\sinh m(d+z)}{\sinh md} \cos(kt - mx) \quad (8)$$

where  $x$  and  $z$  are the horizontal and vertical coordinate directions, respectively,  $m$  is  $2\pi/L$ , and  $k$  is given by

$$k^2 = mg \tanh md \quad (9)$$

Of particular interest is the motion parallel to the bottom surface: When  $z = -d$ ,  $\cosh m(d+z) \rightarrow \cosh(0) = 1$  and Eq. 7 reduces to

$$u = \frac{Hk}{2} \frac{\sin(kt - mx)}{\sinh md} \quad (10)$$

Thus, at the bottom surface beneath a periodic wave, there exists a temporal (periodic) pulsation of velocity. The presence of such a phenomenon could hold great significance in the context of a global flood in explaining the production of local sequences of sedimentary deposits.

It is also of interest to note that, in the higher order theories, there is a net mass-transport associated with traveling waves. Stokes' expression for this transport is of the form

$$\bar{U} = \frac{1}{2} \frac{\pi^2 H^2}{TL} \frac{\cosh \frac{4\pi}{L} (y_0 + d)}{\sinh^2 2\pi d/L} \quad (11)$$

where  $y_0$  is the vertical distance between the still water position and the  $\bar{U}$  vector.

When these fluid velocity fields are present in sediment-laden waters, the many different mechanisms that are present produce a wide variety of depositional patterns. The bedding and lamination characteristics

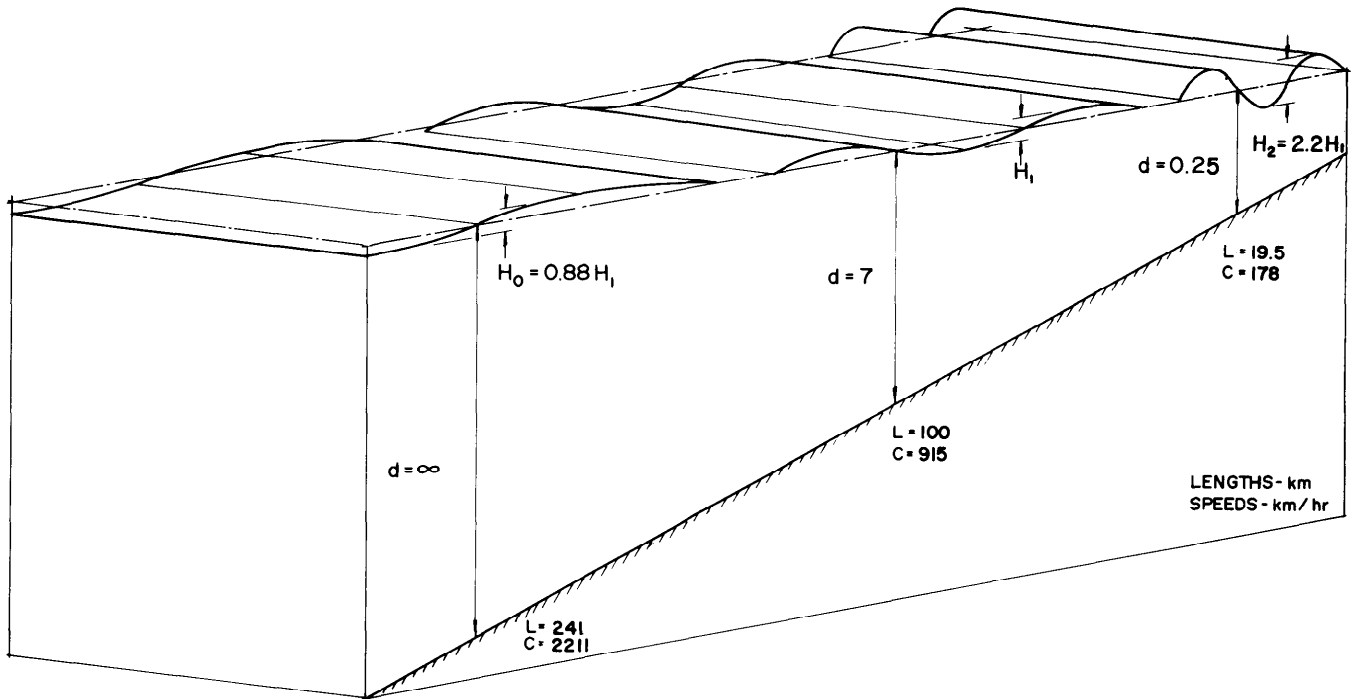


Figure 2. Large-scale periodic waves in waters of various depths. Note that the vertical scale is exaggerated.

observable in the sedimentary rocks result from dune and ripple migration, rolling, sorting, scour, traction, avalanching, and pulsations. The analytical relations of this section give the general characteristics of large scale fluid motions in uniform depth waterways or for special shoaling conditions. When more realistic boundary configurations are to be studied, it is necessary to use numerical analyses to solve for the same types of characteristics.

4. Relevant Theory and Numerical Methodology

All fluid mechanic behavior can be described by the Navier-Stokes (NS) and continuity equations when accompanied by the appropriate initial and boundary conditions. These equations take the form of partial differential equations applicable to each and every differential element in the flow field. Since the lateral motion is not of consequence in the motions to be studied, the two-dimensional versions of these governing equations are sufficient and appear as follows in incompressible flow form:

$$\frac{\partial u}{\partial x} + \frac{\partial v}{\partial y} = 0 \text{ (Continuity)} \tag{12}$$

$$\frac{\partial u}{\partial t} + \frac{\partial u^2}{\partial x} + \frac{\partial uv}{\partial y} = - \frac{\partial p}{\partial x} + g_x + \nu \left( \frac{\partial^2 u}{\partial x^2} + \frac{\partial^2 u}{\partial y^2} \right) \tag{13}$$

(longitudinal (horizontal) NS equation)

$$\frac{\partial v}{\partial t} + \frac{\partial uv}{\partial x} + \frac{\partial v^2}{\partial y} = - \frac{\partial p}{\partial y} + g_y + \nu \left( \frac{\partial^2 v}{\partial x^2} + \frac{\partial^2 v}{\partial y^2} \right) \tag{14}$$

(normal (vertical) NS equation)

where  $u, v$  are the velocity components in the  $x, y$  coordinate directions, respectively,  $t$  is time, and  $\nu$  is the kinematic viscosity. The motion is forced by the terms involving  $p$ , the ratio of pressure to fluid density, and  $g$ , the body acceleration, or by boundary conditions.

Considerable success has been achieved in solving practical, free-surface, transient-flow problems by the Los Alamos Scientific Laboratory of the University of California using the finite-difference, primitive-variable scheme. Starting in the mid-sixties with the Marker and Cell (MAC) method and progressing through various modifications like SMAC and ZUNI in the early seventies, this laboratory issued the SOLA-SURF code in 1975.<sup>2</sup> This code is straight-forward and relatively inexpensive to run, yet is capable of generating solutions to a wide variety of free-surface problems with only minor constraints on the geometrical configuration of the field boundaries. Accordingly, it has been chosen as the vehicle by which the flood simulations will be produced.

By definition, the partial space derivative  $\partial u / \partial x$  (where the velocity component  $u$  is a function of both independent variables  $x, y$  as well as  $t$ ) is given by

$$\frac{\partial u}{\partial x} = \lim_{\Delta x \rightarrow 0} \frac{\Delta u}{\Delta x} \tag{15}$$

As indicated in Fig. 3, the slope of the curve of such a function at a given point can be closely approximated by taking  $\Delta x$  as a small quantity  $\epsilon$  without going to the limit of zero as required by the mathematical definition. Therefore, Eq. (15) can be written

$$\frac{\partial u}{\partial x} \approx \lim_{(x_2 - x_1) \rightarrow \epsilon} \frac{u_2 - u_1}{x_2 - x_1} \approx \frac{u_{i,j}^n - u_{i-1,j}^n}{\Delta x} \tag{16}$$

where  $\epsilon$  is a small quantity, subscripts  $i, j$  are indices in a space grid, and superscript  $n$  is a time index ( $t = n\Delta t$ ).

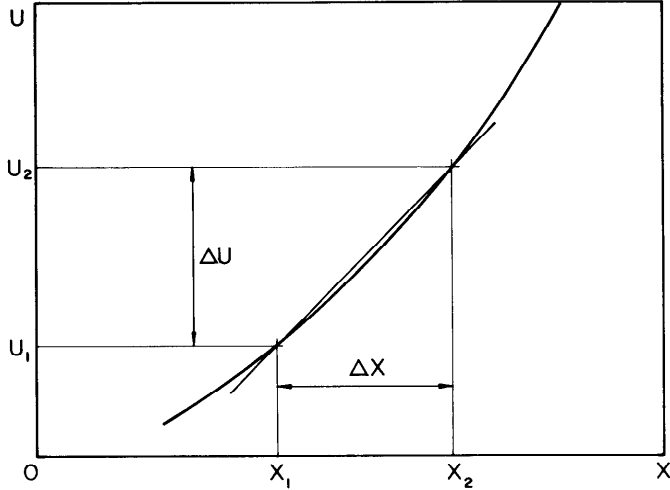


Figure 3. Graphical definition of the partial derivative of  $u$  with respect to  $x$ .

Progressing in a similar manner throughout the individual terms of Eq. (12-14), the governing differential equations can be converted to difference equations. In difference form, the continuity or conservation of mass equation is

$$\frac{1}{\Delta x} (u_{i,j}^{n+1} - u_{i-1,j}^{n+1}) + \frac{1}{\Delta y} (v_{i,j}^{n+1} - v_{i,j-1}^{n+1}) = 0 \quad (17)$$

The NS equations take the following form when solved for the advanced time velocity components

$$u_{i,j}^{n+1} = u_{i,j}^n + \Delta t \left[ \frac{1}{\Delta x} (p_{i,j}^n - p_{i+1,j}^n) + g_x - \text{FLUX} - \text{FLUY} + \text{VISX} \right] \quad (18)$$

$$v_{i,j}^{n+1} = v_{i,j}^n + \Delta t \left[ \frac{1}{\Delta y} (p_{i,j}^n - p_{i,j+1}^n) + g_y - \text{FLVX} - \text{FLVY} + \text{VISY} \right] \quad (19)$$

where a typical convective flux is

$$\text{FLUX} = \frac{1}{4\Delta x} [u_{i,j} + u_{i+1,j}]^2 + \alpha |u_{i,j} + u_{i+1,j}| (u_{i,j} - u_{i+1,j}) - (u_{i-1,j} + u_{i,j})^2 - \alpha |u_{i-1,j} + u_{i,j}| (u_{i-1,j} - u_{i,j}) \quad (20)$$

and a typical viscous flux is

$$\text{VISX} = \nu \left[ \frac{1}{\Delta x^2} (u_{i+1,j} - 2u_{i,j} + u_{i-1,j}) + \frac{1}{\Delta y^2} \cdot (u_{i,j+1} - 2u_{i,j} + u_{i,j-1}) \right] \quad (21)$$

The term  $\alpha$  is a coefficient used to provide various amounts of upwind differencing. If  $\alpha=0$ , centered space differencing is obtained. If appropriately small values of  $\Delta x$ ,  $\Delta y$ , and  $\Delta t$  are selected for use in these equations, they have been shown to yield valid solutions to time-dependent, free-surface problems of practical importance.

### 5. Computer Model

The specification of small spatial and temporal in-

crements of the independent variables requires multitudinous and repetitious application of the governing equations. The digital computer is well suited for such applications provided a systematized code can efficiently range over both the spatial field and temporal period of interest. The general arrangement of spatial meshes is shown in Fig. 4 where rectangular cells of width  $\Delta x$  and height  $\Delta y$  can be individually selected by the I, J indexing system. The actual fluid region is surrounded by a single layer of fictitious cells to aid in the definition of the boundary conditions. Observation of a typical cell (shaded in Fig. 4) shows the exact locations at which the dependent variables  $u$ ,  $v$  and  $p$  are defined.

The same governing equations apply to all flow problems. A given problem is made distinct from the rest by the imposition of the boundary conditions and the forcing function on the specific geometric configuration that describes the field. SOLA-SURF has internal provisions for imposing four different boundary conditions: 1) the free-slip rigid wall for simulating inviscid fluid flows, 2) the no-slip rigid wall for viscous flows, 3) the continuative boundary condition for passing fluid out of the field at a boundary so as to avoid reflective upstream interference, and 4) periodic boundary conditions used to impose a forcing function at a boundary that repeats itself with time. The first two conditions are shown in Fig. 4. The free-slip condition is generated on a horizontal boundary by imposing a  $u$ -component velocity in the fictitious cell equal in magnitude and sign to the  $u$ -component in the cell adjacent to the boundary. The average of these two values produces a slip velocity component of  $u$  at the wall. Since the  $v$ -component is defined at the wall, it can easily be set to zero to complete the free-slip condition. The no-slip condition requires that both  $u$  and  $v$  be zero at the boundary. The  $u$ -component is made zero by imposing in the fictitious cell a  $u$ -component equal in magnitude but opposite in sign to that which occurs in the cell adjacent to the boundary. For vertical boundaries, the roles of the  $u$  and  $v$  components would be interchanged since the  $u$ -component is now defined at the boundary while the  $v$ -component is defined a half mesh away. When the boundaries are curved or slanted, a modification of these definitions is required.<sup>2</sup>

The positions of the free surface, denoted by H, and the bottom surface, denoted by HB, are indexed by JT and JB, respectively, as well as updated during the period of interest by the kinematic equation

$$\frac{\partial H}{\partial t} + u \frac{\partial H}{\partial x} = v \quad (22)$$

At the free surface, the pressure must be zero or a constant value  $p_s$ . The pressure in the cell containing the free surface is chosen so that a linear interpolation between it and the pressure in the cell adjacent below produces a zero value (or  $p_s$ ) at the surface. In equation form,

$$p_{i,JT} = (1 - \eta) p_{i,JT-1} + \eta p_s \quad (23)$$

where  $\eta = \Delta y / [H_i - (JT - 2.5)\Delta y]$

The updated velocity components calculated by Eq. (18) and (19) will not in general, satisfy the continuity condition of Eq. (17). If, for example, there is a net flow of mass into a cell, the cell pressure can be increased to

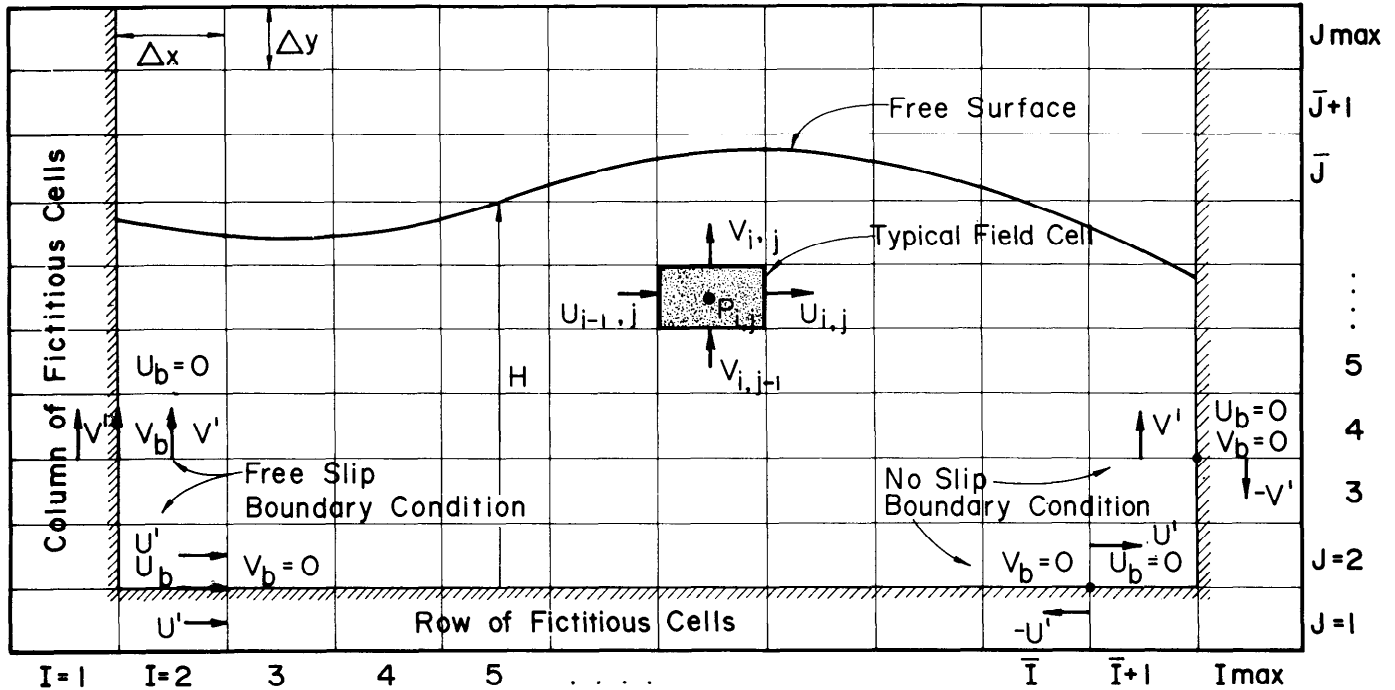


Figure 4. General mesh arrangement showing a typical cell and boundary condition definitions.

decrease the inflow. Contrariwise, when the net flow is out of the cell, the pressure can be reduced to decrease the outflow. The amount of pressure change is given is SOLA by the relation

$$p = -D / \left[ \Delta t \left( \frac{1}{\Delta x^2} + \frac{1}{\Delta y^2} \right) \right] \quad (24)$$

where  $D$  is the divergence obtained when Eq. (17) is calculated (i.e., the amount by which the right hand side deviates from zero). The new cell pressure is then

$$p_{i,j} = p_{i,j} + \Delta p \quad (25)$$

and the velocity components are adjusted to reflect this change,

$$\begin{aligned} u_{i,j} &= u_{i,j} + \frac{\Delta p \Delta t}{\Delta x} \\ u_{i-1,j} &= u_{i-1,j} - \frac{\Delta p \Delta t}{\Delta x} \\ v_{i,j} &= v_{i,j} + \frac{\Delta p \Delta t}{\Delta y} \\ v_{i,j-1} &= v_{i,j-1} - \frac{\Delta p \Delta t}{\Delta y} \end{aligned} \quad (26)$$

These pressure and velocity adjustments must be performed iteratively since the adjustments in one cell affects adjacent cell values. The flow diagram for initiating the calculations and then advancing them temporally through a period of motion is given in SOLA. The temporal advance is governed by the explicit solution of the Navier-Stokes equations for the velocity field once for each cell and for each time step  $\Delta t$ . The adjustment of both velocity and pressure fields is made iteratively using the continuity equation. Iteration is

stopped when a preset allowable divergence is reached; this allowable value being of the order of  $10^{-3}$ .

### 6. Initial Results

In order to gain familiarity with and to test the SOLA-SURF code, a sample problem was run for which a set of correct output values has been established.<sup>2</sup> (See their addendum.) This problem (an undular hydraulic bore) is generated by moving a body of inviscid fluid in a rectangular channel at a uniform velocity into the right-hand rigid boundary. When the fluid interacts with and reflects from the boundary, a wave or bore develops which travels to the left with a characteristic wave form and wave speed. In the test run, the channel was 12 units long (20 meshes at  $\Delta x = 0.6$ ) and 1.6 units high (8 meshes at  $\Delta y = 0.2$ ). Initially, the fluid height was set at  $H = 1.0$  units or 5 meshes. The time step used was  $t = 0.2$ . The bore was maintained with fluid by setting a continuative inflow boundary at the left end of the channel. All other boundaries were given the free-slip condition. The results of the run were in accord with the established output values over a calculation period from  $t = 0$  to  $t = 10$ . See the supplementary illustration.

### 7. Results of Practical Flood Problems

*Solitary Wave on Ramp.* Problems which can be considered germane to Genesis Flood explanations must involve the action of waves or wave trains in regions whose irregular bottom surfaces resemble antediluvial terrain. To initiate the simulations, a single solitary wave (one whose water particles move only in the direction of wave advance) was placed at the beginning of a two-dimensional flow field (10 units high, 27 units long) whose bottom took on an upward slope of 1/5 at a



**Supplementary illustration.** A tidal bore on the Petitcodiac River, near Moncton, New Brunswick, Canada. The calculation of a sort of bore was one of the jobs on which the methods described in this article were tested. The bore shown here is just interesting, not destructive; but one can believe that during the Flood much greater bores may have caused very extensive geological effects.

This picture was supplied by the Department of Tourism of New Brunswick, Fredricton, New Brunswick, Canada, and is used here by permission.

Note the undisturbed water at the right, where the bore has not yet reached, the solitary wave moving to the right, and the disturbed water behind it.

distance of 18 units from the left rigid vertical wall. The right boundary was also rigid and vertical. The solitary wave description given by Laitone<sup>4,5</sup> was used: The surface wave profile in a horizontal channel of constant depth is

$$y_s = d + H \operatorname{sech}^2 (A \omega x - c t) - \frac{3}{4} H \left( \frac{H}{d} \right) \operatorname{sech}^2 (A \omega x - c t) \cdot [1 - \operatorname{sech}^2 (A \omega x - c t)] \quad (27)$$

where

$$A \omega x = \frac{x}{d} \left[ \frac{3}{4} \frac{H}{d} \right]^{1/2} \left[ 1 - \frac{5}{8} \frac{H}{d} \right] \quad (28)$$

and the wave speed

$$c = 1 + \frac{H}{2d} - \frac{3}{20} \left( \frac{H}{d} \right)^2 + \dots \quad (29)$$

The dimensionless velocity field (water particle velocity components normalized by the shallow water wave speed) in a constant-depth channel is given by

$$\frac{u}{(gd)^{1/2}} = \frac{H}{d} \left[ 1 + \frac{1}{4} \frac{H}{d} - \frac{3}{2} \frac{H}{d} \frac{y^2}{d^2} \right] \cdot \operatorname{sech}^2 (A \omega x - c t) + \frac{H^2}{d^2} \left[ -1 + \frac{9}{4} \frac{y^2}{d^2} \right] \cdot \operatorname{sech}^4 (A \omega x - c t) \quad (30)$$

$$\frac{v}{(gd)^{1/2}} = 3^{1/2} \left( \frac{H}{d} \right)^{3/2} \frac{y}{d} \operatorname{sech}^2 (A \omega x - c t) \cdot$$

$$\tanh (A \omega x - c t) \cdot \left[ 1 - \frac{3}{8} \frac{H}{d} - \frac{1}{2} \frac{H}{d} \frac{y^2}{d^2} + \right.$$

$$\left. \frac{H}{d} \left( -2 + \frac{3}{2} \frac{y^2}{d^2} \right) \cdot \operatorname{sech}^2 (A \omega x - c t) \right] \quad (31)$$

The solitary wave selected had a length of 18 units with its center at 9 units from the left end of the field and a maximum height of 1.25 units in a basin whose undisturbed depth was 1.0 units. Since the solitary wave is self-propagating, the flow solution was obtained by imposing the velocity field generated by Eq. (30) and (31) as the initial conditions and the allowing the program to run for a reasonable time. The results of the solution are presented in Fig. 5 in a temporal sequence of surface profiles where a HIDE plot<sup>6</sup> indicates successive traces of the configuration of the free surface as time proceeds. Although the amplitude of the solitary wave increases as it moves up the slope, no secondary waves appear to be generated by the ramp. As the wave reflects from both the right and left boundaries, the amplitude is seen to nearly double. In reflecting, a secondary wave is generated which trails after the main wave, as seen in the rear view representation of Fig. 5, and interferes with it upon reflection off the left end. Although this solution appears to be reasonable, there is no corroborating evidence from the literature to confirm its validity.

*Solitary Wave Moving Towards a Submerged "Continent".* In an effort to simulate a more realistic Flood situation, the solitary wave was next imposed on a field which simulated a continental incline followed, after a maximum rise simulating a coastal mountain range, by an inland basin, all of which were submerged. A somewhat truncated solitary wave (15 units long, center at 4.7 units, height 1.25 units) was placed at the beginning of a 35.4 unit long basin. The first quarter length of the basin bottom was flat, the next quarter had a slope of 1/5, while the last half was described by one wave length of a sine wave which peaked at one-quarter of its length (i.e., at a distance of 21.4 units from the left boundary). The transition from ramp to sine wave was fairly smooth.

The configuration of the free surface is presented in Fig. 6 as a function of time. The movement of the wave up the ramp is without notable incident in the free surface but, as it passes onto the sine wave and over its zenith, a series of secondary waves are generated as seen in the rear view picture. The original wave reflects strongly from the right boundary and considerable interference is observed thereafter as the reflected wave moves back over the inland basin. The generation of the secondary waves is in accord with occurrences in similar calculations. For example, Kim and Lee<sup>7</sup> have shown the transformation of a solitary wave into a series of waves as motion was calculated up a ramp and into a channel half the original height. The generation of these extra waves could hold added meaning in the explanation of sedimentary layering due to wave action.

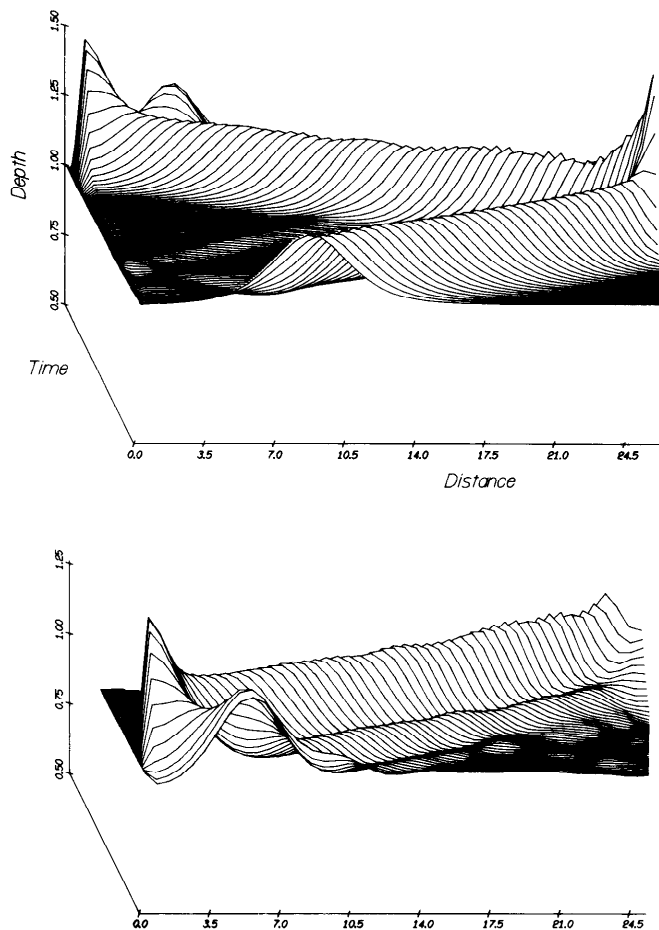


Figure 5. Temporal sequence of free-surface configurations as a solitary wave moves up a ramp. Upper part, front view; lower, rear view. This calculation was made for zero viscosity.

Additional information regarding the water action connected with the passage of the solitary wave can be obtained from examination of the velocity fields at various times during the course of the motion. In Fig. 7 is shown a temporal sequence of velocity vector plots for this "continent" configuration. The  $u$  and  $v$  component velocities as calculated were averaged in such a way as to redefine the velocity components at the center of each cell. They were then added vectorially and plotted to an appropriate scale. Since the calculations were made for a fluid with zero viscosity and for the free slip boundary conditions, the vector plots reflect these stipulations. Some of the features noted in Fig. 6 can be observed in this type of plot as well, the most striking being the transformation of the solitary wave into a series of waves once the zenith of the bottom boundary's sine wave is encountered. The classic velocity field of the solitary wave at the beginning of the sequence is seen to undergo dramatic changes on the ramp and sinusoid. Worthy of note is the observation that the secondary waves move at a greatly reduced wave speed.

This set of calculations was made with an undisturbed free surface height of 1.0 units and a sinusoid amplitude of 0.4. This combination provided a reasonable amount of water on top of the zenith of the sinusoid as well as a flooded inland basin. On another

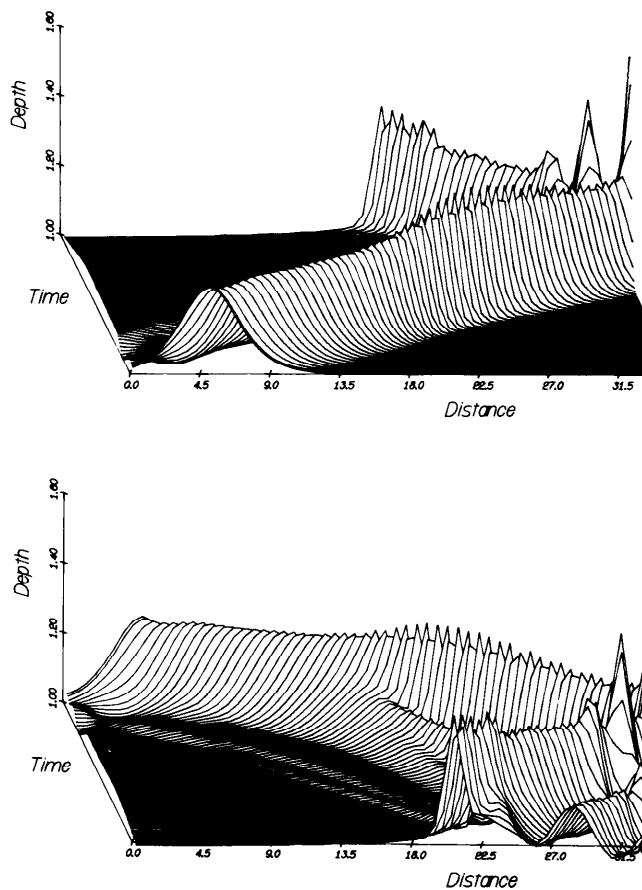


Figure 6. Temporal sequence of free-surface configurations as a solitary wave moves toward a submerged "continent". Upper part, front view; lower, rear view. This calculation was made for zero viscosity.

trial, the sinusoid amplitude was set at 0.2 which made the undisturbed free surface just intersect the zenith of the sinusoid for an undisturbed depth of 1.0 units. For the most part, the results of these calculations paralleled those shown in Fig. 7. However, the SOLA-SURF code could not resolve the difficulty encountered with the inadequate amount of fluid at the zenith of the sinusoid. Further study of this type of situation is needed and quite possibly a stronger code will be required to handle this special boundary condition.

*Subaquatic Activity—Water Injection Through the Bottom Boundary.* The final two attempts at mimicking flood situations in this initial study were aimed at investigating the fluid dynamic events associated with the welling-up of fluids from beneath the free surface as could be produced by a subaquatic earth movement with or without subsequent issuance of water through the disturbed bottom boundary. The idea for this simulation arises from a consideration of Gen. 7:11 where it states that in the 600th year, the second month, and 17th day of Noah's life "the fountains of the great deep" were broken up. In any valid analysis of the Genesis Flood, it must be realized that a considerable percentage of the water could have come from such a source. Questions arise as to the consequences of such

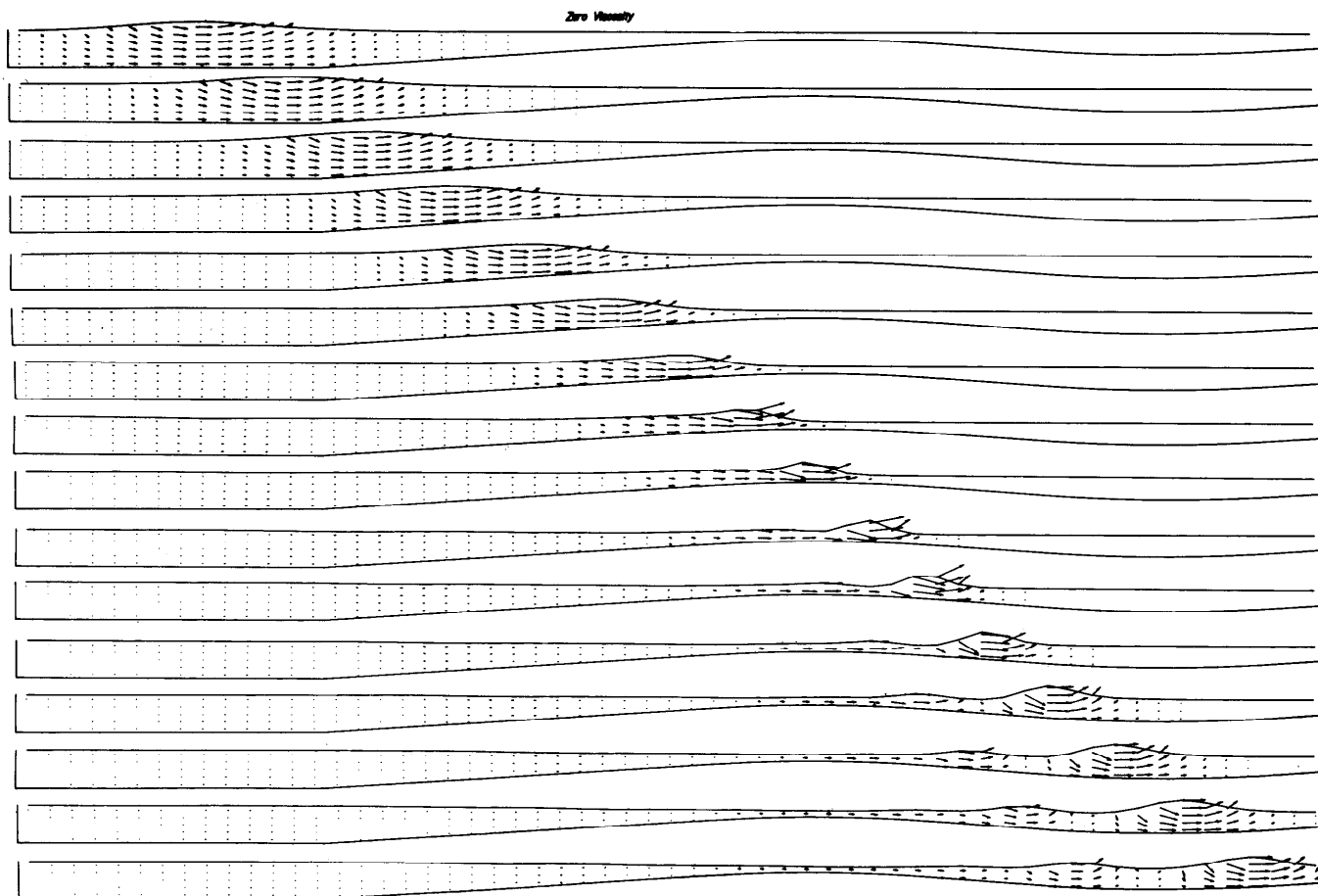


Figure 7. Temporal sequence of velocity vector field plots as a solitary wave moves toward a submerged "continent". This calculation was made for zero viscosity. The sequence reads from the top down.

events: how are such occurrences manifested on the surface? are wave motions developed? what velocity fields are produced in the vicinity? etc. A simplified representation of a "fountain" can be developed by using a portion of the bottom boundary of the basin as a "source" region where fluid is allowed to enter the field. As can be seen in the right half of Fig. 8, a rectangular field 12 units long, initially filled with quiescent fluid, was subjected to an upward ( $v$  component only) velocity at the boundary between 3 and 6 units. This upward flow was continued for a period of 6 seconds after which the "fountain" was turned off. This action activated the whole flow field as can be seen in Frames 2-4 in Fig. 8. The first manifestation on the surface was the welling-up of the fluid directly over the site of the bottom opening with fluid being given lateral motion on both sides of the source. The complexity of the fluid action was increased by the reflection of these waves off from both left and right rigid vertical walls. Once the incident waves were reflected, they in turn interacted and interfered with each other as the motion continued to develop. This sequence, calculated with no slip boundaries and a water viscosity, differs only in details from a second sequence (not shown) in which free slip and zero viscosity were stipulated.

Another variant of this type of calculation is shown in the left half of Fig. 8 where the length of time during

which the "fountain" was issuing fluid was increased to coincide with the total time of program run. The action in the field and at the surface is similar to the short opening time but is somewhat more dominated by the presence of the "fountain". The total volume of fluid increases considerably by the end of the sequence as well.

The configuration of the free surface as a function of time for both the short and long openings for the viscid cases are presented in Fig. 9. The interaction of the incident and reflected waves generated by the subaquatic source is dramatically illustrated.

*Subaquatic Activity*—Upheaval of the Bottom Boundary. The welling-up of water in a localized region could also be accomplished by an upward movement of the bottom boundary itself. If this movement took place rapidly, the fluid would be carried upward congruently with the boundary. In the simulation shown in Fig. 10, a field length of 18 units was used in which that section of the bottom boundary between 4 and 10 units was given an upward velocity corresponding to the temporal versine displacement generated by the following equation:

$$HB(I) = \frac{\epsilon_0}{2} \cdot \sin \left( \frac{2\pi T}{\sigma} \right) \left( 1 - \cos \left( \frac{2\pi X(I)}{L} \right) \right) \tag{32}$$

where HB(I) is the local displacement of the bottom at

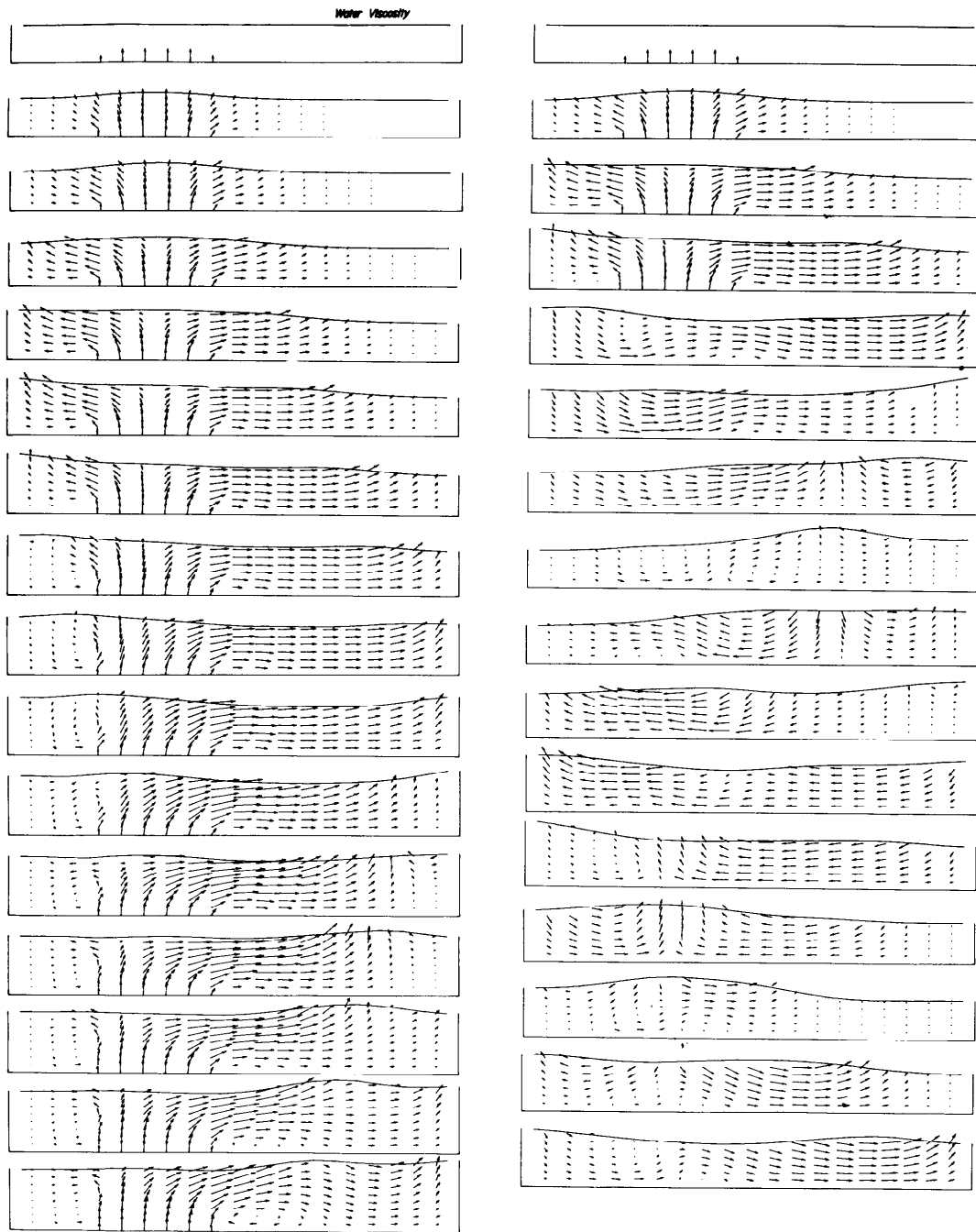


Figure 8. Temporal sequence of velocity vector field plots for a basin with water injection through the bottom boundary. Left, long opening; right, short opening. Water viscosity was used in the calculation. The sequence reads from the top down.

the  $i$ th section of the channel,  $\epsilon_0$  is the maximum upward displacement of the bottom boundary,  $\sigma$  is a parameter governing the period of the boundary motion, and  $L$  is the length of the 6-unit versine section. A series of  $\sigma$ -values were used to explore the phenomenon; the  $\sigma=10$  value used in the display in Fig. 10 and 11 moved the bottom boundary suddenly enough to carry the water upward without running off during the process. During the quarter period of motion generated, the bottom was raised to its maximum amplitude of 0.5 units corresponding to the 10th time frame in Fig. 10.

After reaching this position, the motion of the boundary was stopped.

As can be seen from this sequence of velocity vector fields, the water then begins to flow down from this rise in the bottom boundary. In so doing, two rather large waves develop at the ends of the versine which in due time begin to propagate away from the rise. After several reflections from the rigid vertical walls at both left and right ends of the basin, the motion eventually dies down and the free surface adopts a nearly horizontal position in Frame 84. With additional computer

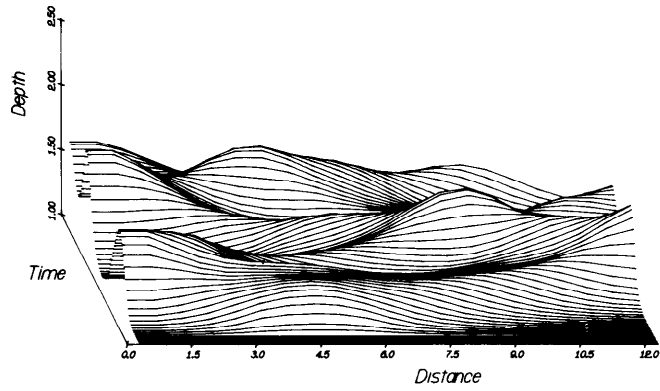
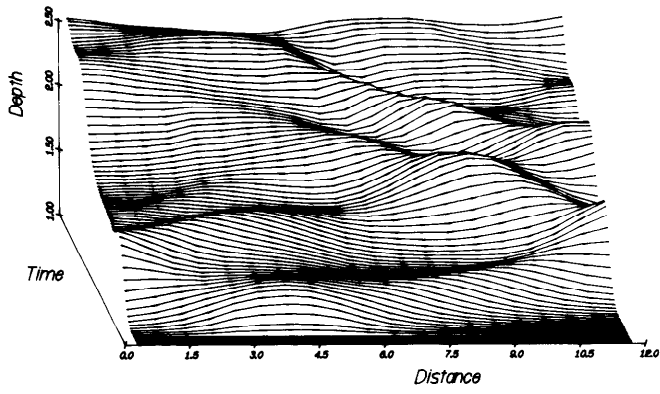
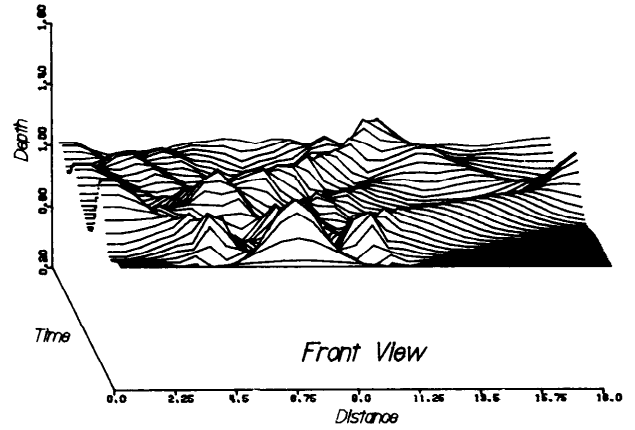
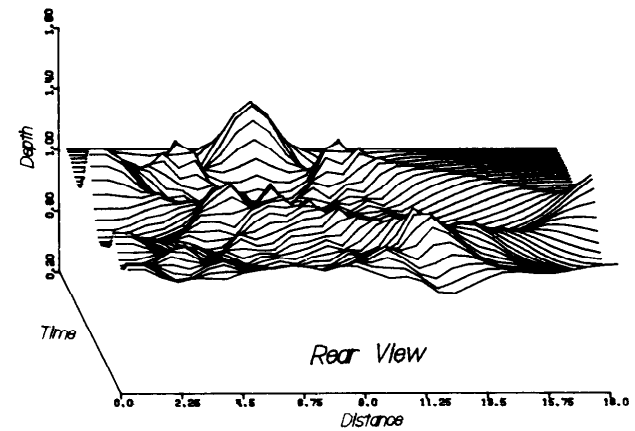


Figure 9. Temporal sequence of free-surface configurations for bottom boundary water injection. Above, long opening, front view; below, short opening, front view. Water viscosity was used in the calculation



$\epsilon_0 = 0.5$     $\sigma = 10.0$    Water Viscosity



$\epsilon_0 = 0.5$     $\sigma = 10.0$    Water Viscosity

Figure 11. Temporal sequence of free-surface configurations for bottom boundary upheaval. Water viscosity was used in the calculations.

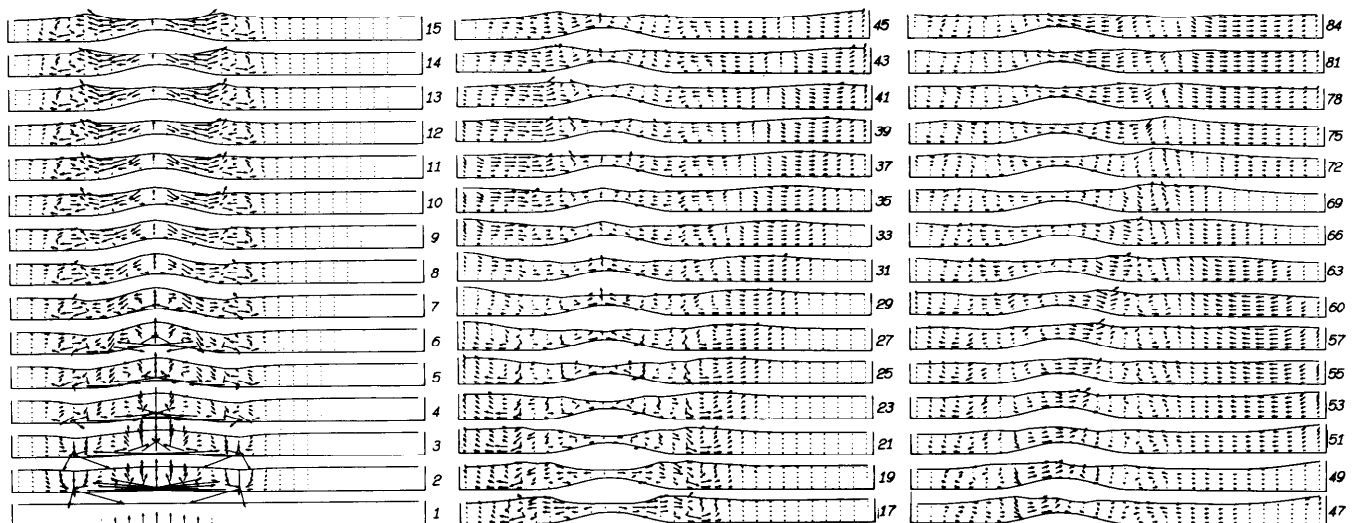


Figure 10. Temporal sequence of velocity vector field plots for a basin with upheaval of the bottom boundary. The sequence is shown by the numbers.

running time, the fluid motion still present in Frame 84 would be stopped by the viscous action and the free surface would be horizontal over the quiescent basin of water.

Of particular note is the considerable amount of fluid activity that occurs throughout the time sequence but particularly during the boundary motion. The large vortices, developed at the ends of the versine, decay slowly. The waves mentioned before have similar characteristics to the solitary waves imposed by equations in Fig. 5 and 6. The initial development of the free surface during uplift as well as subsequent propagation, reflection, and interference effects are clearly delineated by the temporal sequence of free-surface configurations shown in Fig. 11.

### 8. Discussion and Conclusions

The hypothesis adopted in this study reveals the authors' beliefs that the Genesis Flood was a dynamic year-long historical event that shaped the character of the earth's crust into the form we now see. These beliefs originated at the level of a literal interpretation of Scripture and have been augmented and confirmed by various subsequent studies including the one presented herein. The large water mass that prevailed during that period of history was anything but tranquil due to the variety of spatially- and temporally-varying forces that were brought to bear upon it. During the early stages, these forcing functions, which included large tectonic movements, the releasing of the "fountains of the deep", and large-scale hydro-thermal activity, were continuous although erratic and caused wave motions which were subsequently amplified by wave reflections and interference. The persistence of these perturbations during that period of the flood when the earth was completely covered with water led to enhanced cyclic activity since the wave motions were not readily damped because of the spherical geometry of the ocean system.

Yet to be quantitatively considered in all this dynamic activity is the contribution due to the gravitational forces caused by the earth-moon and earth-sun attraction. The frequency of the resulting semi-diurnal tide (12 hr.) is known to be close to the natural frequency of a global ocean for some modes of oscillation.<sup>8</sup> It is reasonable to assume that the normally-small present-day tidal effects could be greatly amplified due to resonance. The reasonableness of assuming that the tidal effects during the flood year were greatly augmented is increased when it is realized that the governing parameters associated with tidal resonance effects would be quite different from present-day values. Hendershott says "This proximity to semi-diurnal resonance should not be surprising in view of the rich spectrum of free oscillations possible in even a regular flat-bottom ocean of global extent. —Variable bottom relief introduces additional free oscillations".

Also adopted in this study is the concept that the sedimentary structures which exist in the geologic record show cyclic characteristics as well as persistence over vast continental regions. These observations are in keeping with the aforementioned global and continental wave motions. Coupled with these observations are the uniform depositional characteristics of the sedimen-

tary layers without erosional channels and cuts to indicate intermediate passage of time. If the slow motions of local flood waters involving many millenia were responsible for the deposition of the geologic column, as is specified in uniformitarian geology, no two sedimentary strata should be seen in complete conformity. Rather, the sequence should show the evidence of continual interruptions in the layering process and a general lack of strata conformity.

Furthermore, there is Scripture support for the dynamic nature of the flood. Gen. 7: 18-19 states that "the waters prevailed and were increased greatly upon the earth—and the waters prevailed exceedingly upon the earth." Since the concepts of strength, vehemence, and insolence are involved in the words "prevailed exceedingly (*gahar meod*)", it can be inferred that dynamism rather than tranquillity was extant. After the 40 initial flood days in which both the "windows of heaven" and "fountains of the deep" were active, there were 150 days in which "the waters returned from off the earth continually" (Gen. 8: 3). Nelson<sup>9</sup>, instead of rendering "*halak*" as "continually", finds evidence for a more literal translation of "to and fro." He discusses this interpretation and gives other Scriptural support for a flood characterized by large motions and strong forces. New Testament writers (Mt. 24:39, Lk. 17: 27, 2 Pet. 2: 5, 3: 6), when referring to this historic event consistently use a unique word (*kataklusmos*) for the flood. It is the word translated in the Greek (and English) as "cataclysm." Again, it is easy to infer the dynamic character of the flood as opposed to a tranquil one.

In depicting the flow fields associated with several practical Genesis Flood situations, it has been shown that it is possible using numerical analysis to simulate the motions of large bodies of water having irregular boundary geometries and complex initial and boundary conditions. Considerable free surface activity has been demonstrated but, equally as important, significant temporal and spacial velocity distributions have been shown to occur in close proximity to the bottom boundary. These distributions are essential if these flows are to be capable of developing bed forms similar to the many sedimentary layers and cycles of rock units found throughout the world. For the large number of sedimentary layers to be deposited during the flood year instead of during the countless millenia available according to uniformitarian notions, there would need to be daily occurrences of mechanisms capable of producing large waves. Resonating tidal waves (i.e., tidal waves that have large amplitudes) could twice daily produce large moving masses of fluid capable of bringing bed loads into position for deposition once the wave passed. Interference effects associated with these waves would multiply the number of deposits that could be laid down per day. Since subaquatic mechanisms of the types investigated herein could have been frequently imposed during the early stages of the flood year, these too could have contributed greatly to the wave activity and the concomitant sedimentary environment. The difficulty and computer effort of the modeling would increase many fold if the particulate matter were included. Although attempts at such modeling are contemplated, the alternative of physically modeling the sedimentary

process is already in progress.<sup>1</sup> The coupling between the computer modeling and the physical modeling should increase the likelihood of arriving at a plausible physical explanation of geological features in accord with Scriptural accounts of the Genesis Flood.

### References

- <sup>1</sup>Voss, H.D., M.E. Clark, R. Taubold, J. Osterbur, T. Dalton, and E. Gruschow, 1980. Investigation of a global flood using a large circular flume. In preparation.  
<sup>2</sup>Hirt, C.W., B.D. Nichols, and N.C. Romero, 1975. SOLA—a numerical solution algorithm for transient fluid flows. Los Alamos Scientific Lab., Rept. LA-5852.

- <sup>3</sup>Wiegel, R.L., 1964. Oceanographical engineering. Prentice-Hall.  
<sup>4</sup>Laitone, E.V., 1959. Water waves IV, shallow water waves. University of California Engineering Research Technical Report 82-11.  
<sup>5</sup>Laitone, E.V., 1960. The second approximation to cnoidal and solitary waves. *Journal of Fluid Mechanics* 9, part 3, 430-444.  
<sup>6</sup>Williamson, H., 1972. Hidden-line plotting program. *Communications of the A.C.M.* 15 (2): 100-103.  
<sup>7</sup>Kim, S.T., and J.J. Lee, 1977. Numerical solutions of viscous KdV equations—application in water waves. (In) *Proceedings of the Symposium on Applications of Computer Methods in Engineering* (Ed. L.C. Wellford, Jr.) 1, 347-355.  
<sup>8</sup>Hendershott, M.C., 1973. Ocean tides. *EOS, Transactions of the American Geophysical Union* 76-86.  
<sup>9</sup>Nelson, B.C., 1931. The deluge story in stone. Bethany Fellowship, Inc. Publishers, Minneapolis.

## THE WARM EARTH FALLACY

GLENN R. MORTON\*

Received 11 June, 1979

*An analysis of the assumptions which must be made when ancient climate is inferred from the fossil record reveals that one must accept the Principle of Uniformitarianism and quite possibly the Theory of Evolution in order to determine the climate. Under the assumption that the earth has undergone a worldwide flood of a year's duration, it is impossible to determine what the pre-flood climate was like. The implications of this are that all current flood models which attempt to satisfy the warm earth criteria may be satisfying a situation which never existed.*

For over fifty years one of the most firmly accepted creationist doctrines has been that the earth before the flood had a uniformly mild climate. Whitcomb and Morris have no less than eight quotations from three authorities attesting to the universal warmth of various ancient geologic periods.<sup>1</sup> Smith presents evidence in favor of the warm earth theory.<sup>2</sup> Rehwinke<sup>3</sup> as well as Whitcomb and Morris cites coal as evidence of the warmth of the prediluvial world. In fact Whitcomb and Morris state that,

"A universal warm, moist climate alone explains the evidence."<sup>4</sup>

Dillow cites limestone deposits in the higher latitudes, palm trees in Alaska, crocodiles in New Jersey, and frozen ripe fruit found in the New Siberian Islands as evidence of this mild climate. In fact he makes a temperature estimate of the pre-flood world based upon the fossils found at various latitudes.<sup>5</sup>

Other examples are easily brought to mind. Fossil tropical breadfruit found, along with magnolias, laurels, ferns, and sequoias, 300 miles north of the Arctic Circle.<sup>6</sup> The Byrd expedition discovered fossil ferns at latitude 87° S.<sup>7</sup> Obviously, such facts strongly compel a researcher to accept the idea that the polar regions were considerably warmer in the past than they are presently. There just seems to be no way any such animals and plants could have lived in these regions under present climatic regimes.

However, an analysis of the assumptions which one must make to determine the pre-flood climate shows that they are totally incompatible with the assumption

of a worldwide flood. The reason for this is that in order to infer climate from the fossil record one must implicitly accept the Principle of Uniformitarianism.

Two assumptions must be made before climatic information can be deduced. First, it must be assumed that the habitats of the fossil species being studied are of the same kind as can be observed to be inhabited by the living representatives today. In other words, the habitat has not changed. This is the first form of this assumption. When the case occurs that there are no living representatives in a fossil assemblage, it must be assumed that the habitat is similar to that of the nearest living "relatives". This is the second form of the first assumption. Few creationists would have problems accepting it in its first form; but they should feel uncomfortable with its second form. In accepting it in its second form as stated, one is implicitly accepting evolution; because only in the theory of evolution are there any relatives! One could escape this by assuming that God created similar forms to occupy similar environments, but he must be careful in making this assumption. With the wide climatic tolerances observed within various genera, this assumption is shaky at best.

It is only by using this second form that any climatic inferences can be made, e.g. from dinosaurs. There are no living representatives; but the reptiles, being structurally similar to these ancient creatures (although this has been questioned) are used as the models. Thus it is concluded that the dinosaurs must have been cold-blooded and lived in more temperate climes. By this reasoning, then, the dinosaur footprints on Svalbard means that the area was once warm.<sup>8</sup> Accepting this conclusion is uncomfortably close to accepting evolution also.

\*Mr. Glenn R. Morton lives at 3313 Clavmore, Plano, Texas 75075.